Available online at www.sciencedirect.com
ScienceDirect
Bioorganic & Medicinal Chemistry Letters
Bioorganic & Medicinal Chemistry Letters 17 (2007) 3618–3623

1,4-Dihydroindeno[1,2-*c*]pyrazoles as potent checkpoint kinase 1 inhibitors: Extended exploration on phenyl ring substitutions and preliminary ADME/PK studies

Yunsong Tong,* Akiyo Claiborne, Magdalena Pyzytulinska, Zhi-Fu Tao, Kent D. Stewart, Peter Kovar, Zehan Chen, Robert B. Credo, Ran Guan, Philip J. Merta, Haiying Zhang, Jennifer Bouska, Elizabeth A. Everitt, Bernard P. Murry, Dean Hickman, Tim J. Stratton, Jian Wu, Saul H. Rosenberg, Hing L. Sham, Thomas J. Sowin and Nan-horng Lin

Cancer Research, Global Pharmaceutical R&D, R47S, AP10, Abbott Laboratories, 100 Abbott Park Road, Abbott Park, IL 60064, USA

Received 12 March 2007; revised 13 April 2007; accepted 17 April 2007
Available online 25 April 2007

Abstract—A study on substitutions at the four open positions on the phenyl ring of the 1,4-dihydroindeno[1,2-*c*]pyrazoles as potent CHK-1 inhibitors is described. Bis-substitution at both the 6- and 7-positions led to inhibitors with IC_{50} values below 0.3 nM. The compound with the best overall activities (**36**) was able to potentiate the anti-proliferative effect of doxorubicin in HeLa cells by at least 47-fold. Physicochemical, metabolic, and pharmacokinetic properties of selected inhibitors are also disclosed.

The concept of sensitizing cancer to the effects of DNA-damaging agents through inhibition of checkpoint kinase 1 (CHK-1) has been well established.[1] CHK-1 is activated via phosphorylation by its upstream kinases ATR and/or ATM upon DNA damage, leading to phosphorylation and degradation of CDC25A. The downstream event is the inhibition of cyclin E/Cdk2 or cyclin B/Cdc2 kinases, which ultimately causes cell cycle arrest at S or G2/M phase.[2] The effectiveness of the DNA-damaging agents faces deterioration since the *p*53-deficient cancer cells have a mechanism of repairing themselves at the S or G2/M phases. Therefore, inhibition of CHK-1 to abrogate S and/or G2/M checkpoints can drive cancer cells into premature mitosis and apoptosis. On the other hand, the DNA-damaging agents have little impact on normal cells since they have the ability to arrest through *p*53-mediated G1 checkpoint.[3]

Recently, we disclosed a new class of 1,4-dihydroindeno[1,2-*c*]pyrazole compounds as potent and selective CHK-1 inhibitors (Chart 1).[4] Our early study was focused on investigating the structural biology of this class of molecules. We learned that key extra hydrogen bondings between the phenolic alcohol (or corresponding carboxylic acid) of the inhibitors to the polar region of the kinase in the active site were needed for high potency, in addition to the bidentate hydrogen bonding between the pyrazole part of the molecules and the hinge region of the kinase. However, the substitution on the phenyl ring of the tricyclic pyrazole core was limited at the 6-position with narrow variations. In this paper, we explore the expanded substitution types and positions around the fused phenyl ring while keeping the bi-aryl phenol at the 3-position. In addition, we disclose the metabolic, physicochemical, and pharmacokinetic (PK) profiles of selected potent inhibitors and our initial attempt to optimize the PK properties.

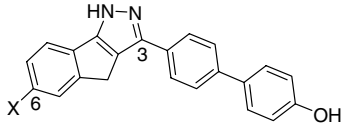

Chart 1.

Keywords: 1,4-Dihydroindeno[1,2-*c*]pyrazoles; Checkpoint kinase 1 inhibitors; Chk-1 inhibitors; Sensitizing DNA-damaging agents.
* Corresponding author. Tel.: +1 847 935 1252; fax: +1 847 935 5165; e-mail: yunsong.tong@abbott.com

0960-894X/$ - see front matter © 2007 Elsevier Ltd. All rights reserved.
doi:10.1016/j.bmcl.2007.04.055

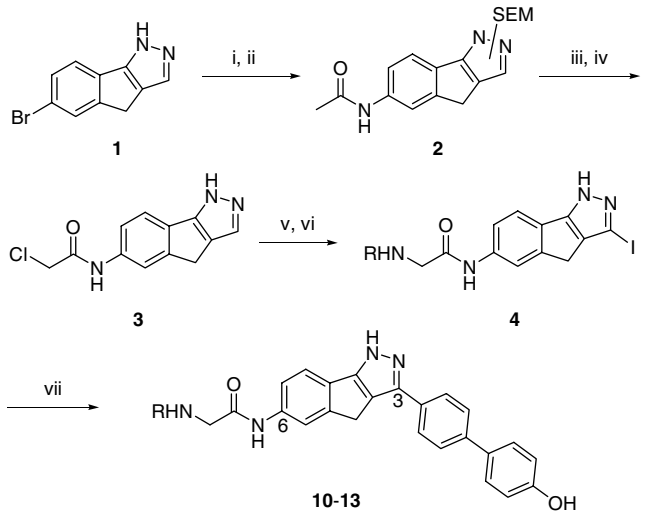

Scheme 1. Reagents and conditions: (i) NaH, SEMCl, DMF, 100%; (ii) $Pd(OAc)_2$, Xantphos, Cs_2CO_3, acetamide, 1,4-dioxane, 100 °C, 79%; (iii) HCl, MeOH, 100%; (iv) $NaHCO_3$, chloroacetyl chloride, acetone, 78%; (v) NIS, DMF, 75 °C, 43%; (vi) amines, EtOH, or DMF, 50–100%; (vii) 4-biphenol pinacol borate, $Pd(PPh_3)_2Cl_2$, Na_2CO_3, EtOH/DME/H_2O, microwave, 170 °C, 500 s, ~20–40%.

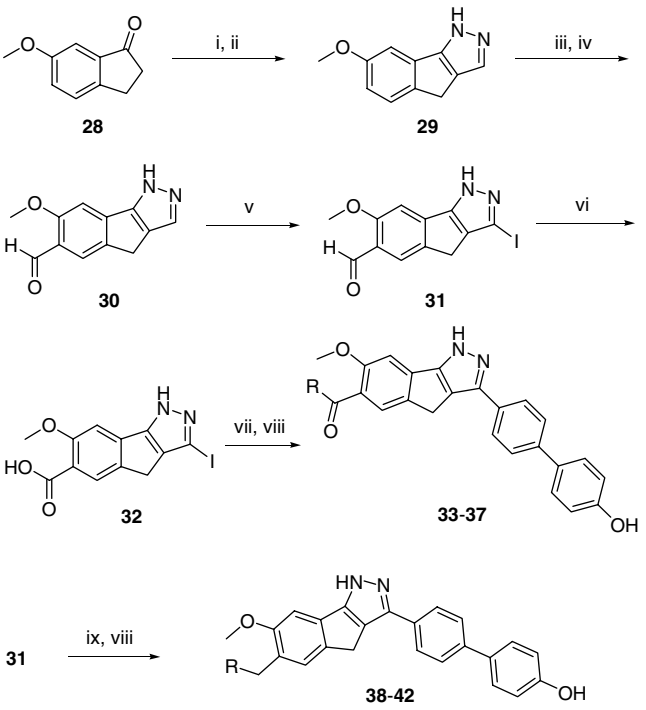

Scheme 2. Reagents and conditions: (i) NaH, ethyl formate, benzene, 91%; (ii) NH_2NH_2, AcOH, 90 °C, 84%; (iii) Br_2, AcOH, 95%; (iv) PhLi, *s*-BuLi, THF, DMF, −78 °C to rt, 99%; (v) NIS, DMF, 80 °C, 68%; (vi) $NaClO_2$, KH_2PO_4, NH_2SO_3H, H_2O/1,4-dioxane, 65%; (vii) 1° amines, EDC, HOBt, Et_3N, DMF, rt; or 2° amines, PyBOP, DIEA, DMF, rt; (viii) 4-biphenol pinacol borate, $Pd(PPh_3)_2Cl_2$, Na_2CO_3, EtOH/DME/H_2O, microwave, 160–180 °C, 600–1000 s, ~16–37%; (ix) a—amines, TsOH, toluene, reflux; b—$NaBH_4$, EtOH, THF.

Scheme 1 outlines how compounds **10**–**13**, carrying an acetylamino linker at the 6-position, were synthesized. The pyrazole portion of the known compound **1**[5] was protected by SEM and the acetyl amino group was introduced at the 6-position following a Buchwald protocol[6] to give **2**. Both the acetyl and the SEM groups were removed with HCl. The aniline nitrogen was subsequently converted to the chloroacetamide. The resulting compound **3** was iodonated at the 3-position using NIS followed by nucleophilic substitution with various amines to complete the side-chains at the 6-position. The bi-aryl phenol was then installed via a Suzuki coupling providing **10**–**13**.

The synthesis of bis-substituted compounds **33**–**42** is shown in Scheme 2. 6-Methoxy-1-indanone **28** was treated with NaH and ethyl formate followed by pyrazole ring closure in the presence of hydrazine and acetic acid. Compound **29** was lithiated and treated with DMF to afford the aldehyde **30**. Iodonation using NIS gave **31**. The formyl group at the 6-position was oxidized to the carboxylic acid, which was in turn converted into an amide using either HOBT/EDC or PyBOP coupling conditions. The bi-aryl phenol unit was introduced in the final step to complete the synthesis of **33**–**37**. Meanwhile, reductive amination on the formyl group of **31** followed by Suzuki coupling afforded compounds **38**–**42**.

The synthesis of **48** (Scheme 3) with a gem-dimethyl group at the 4-position of the tricyclic core started with **43** prepared via a known protocol.[7] The phenolic alcohol of **43** was protected with a SEM group followed by pyrazole formation to provide **44**. Protection of the pyrazole nitrogen and selective removal of the SEM on the phenol gave **45**. The resulting hydroxyl group was converted into an amide via a triflate intermediate with good yield. The remaining transformations were completed using well-developed chemistry resulting in **48**. The yield for the final Suzuki coupling step was much higher if the pyrazole nitrogen was protected. The synthesis of compounds **49**–**52** (Scheme 4) was similar to the procedures reported earlier.[4]

Our earlier work on 1,4-dihydroindeno[1,2-*c*]pyrazoles[4] had limited substitution patterns on the phenyl ring of the tricyclic core since all of the inhibitors carried extended side-chains with either an aminomethyl or an aminocarbonyl linker at the 6-position, exemplified by **6** or **7** (Table 1). As indicated in the same table, a smaller substitution such as a hydroxyl or a hydroxymethyl showed similar potency. Both **8** and **9** possessed IC_{50} values below 10 nM. However, the unsubstituted compound (**5**) suffered a dramatic potency loss (IC_{50} = 1373 nM). Compounds having side-chains linked by an acetylamino group (**10**–**13**) uniformly performed well in the enzymatic assay. With an IC_{50} value at 0.74 nM, inhibitor **13** was the most potent compound containing a 6-position substitution.

We also investigated substitutions on the remaining three open positions (5, 7, and 8) of the phenyl ring with results displayed in Table 2. Within the CHK-1 binding pocket,[10] the substitution at the 5-position is sandwiched by protein walls with a narrow opening. The small groups were well tolerated at the 5-position as

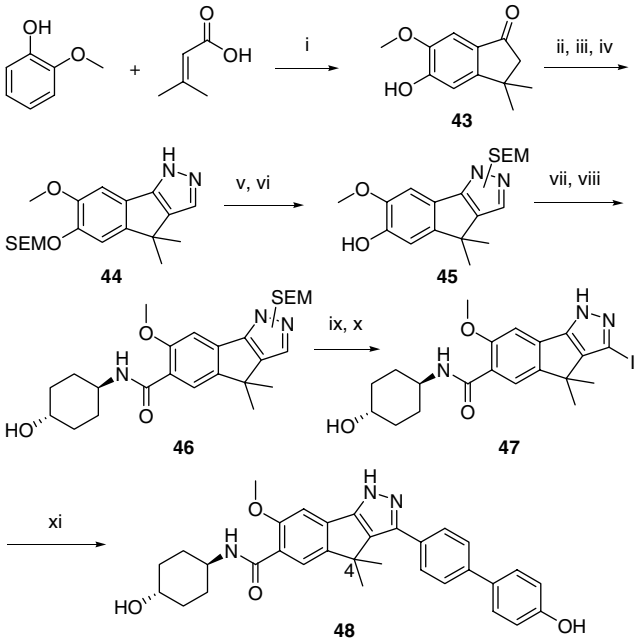

Scheme 3. Reagents and conditions: (i) polyphosphoric acid, 40–110 °C, 39%; (ii) SEMCl, DIEA, CH_2Cl_2, 93%; (iii) NaH, ethyl formate, THF, 50 °C, 74%; (iv) NH_2NH_2 monohydrate, AcOH, EtOH, 85 °C, 89%; (v) SEMCl, NaH, THF, 95%; (vi) HCl, MeOH, 50%; (vii) $PhN(OTf)_2$, NaH, THF, 40 °C, 96%; (viii) CO, $PdCl_2(dppf)\cdot CH_2Cl_2$, *trans*-4-aminocyclohexanol, THF, TEA, 245 psi, 120 °C, 77%; (ix) HCl, EtOH, 60 °C, 50%; (x) NIS, 1,4-dioxnae, 90 °C, 34%; (xi) 4-biphenol pinacol borate, $Pd(PPh_3)_2Cl_2$, Na_2CO_3, EtOH/DME/H_2O, microwave, 180 °C, 1000 s, 7%.

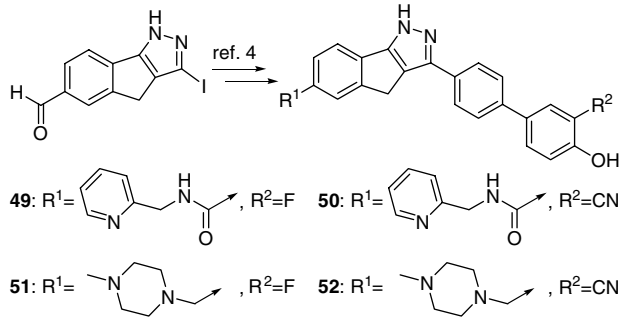

Scheme 4.

14 and **15** possessed IC_{50} values between 5 and 8 nM. However, the potency deteriorated upon increasing the size of the substitution. As such, compound **16** suffered a greater than 20-fold drop in its activity, while **17** and **18** with long and bulky side-chains completely lost potency. Substitutions at the 7-position are outside of the binding cavity and extended into the solvent similar to those at the 6-position. Consequently, groups with variable size and length all resulted in potent inhibitors (**19**–**26**) with IC_{50} values ranging from 2 to 34 nM. The 8-position is very close to the protein backbone in the active site and was not considered to be an ideal site for the SAR study. Compound **27** with a hydroxy group in that position was a much weaker inhibitor with an IC_{50} value of 671 nM as anticipated.

Table 1. Substitutions at 6-position: extended study

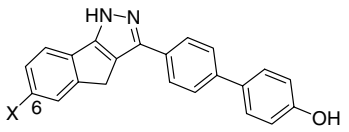

Compound	X	CHK-1 IC_{50}[a] (nM)
5	H	1373
6	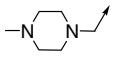	24
7	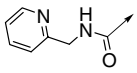	9.3
8[8]	OH	4.4
9[8]	CH_2OH	7.7
10	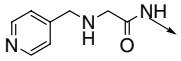	6.4
11	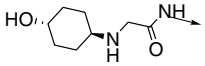	1.2
12	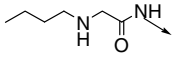	2.1
13	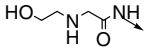	0.74

[a] Compound concentration needed to cause 50% inhibition of Cdc25C phosphorylation in the presence of recombinant CHK-1 protein (ATP concentration is 5 μM).[9]

Interestingly, substitutions at both the 6- and 7-positions appeared to have some additive effect. As shown in Table 3, a methoxy group at the 7-position coupled with a solubilizing group at the 6-position led to compounds with IC_{50} values mostly less than 1 nM (**33**–**42**). For the most potent compounds, **33**, **36**, and **40**, the IC_{50} values were in the range of 0.2–0.3 nM, which represents at least a 10-fold improvement over most of the mono-substituted inhibitors. While both 6- and 7-positions are solvent exposed, the 7-position is closer to the protein. The 7-OMe group can bind to the enzyme by making van der Waals contact within a small hydrophobic pocket formed by the side-chain of Tyr86 and the methylene of Gly90. We speculate that the presence of the 6-substitution may limit the 7-OMe group to be conformationally organized into the requisite binding orientation and resulted in inhibitors with superior potency.

Potent inhibitors in the enzymatic assay were further evaluated in a functional and a mechanism-based cellular assay.[11] The functional assay was a cell proliferation assay (MTS assay) in HeLa cells. In this assay, the anti-proliferation effect was measured in the form of EC_{50} values for a CHK-1 inhibitor as a single agent and also

Table 2. Substitutions at 5-, 7-, or 8-position[a]

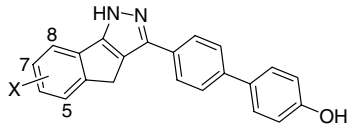

Compound	X position	X	CHK-1 IC_{50} (nM)
14	5	Acetylamino	5.5
15	5	CH_2OH	7.8
16	5	2,2-Dimethyl-propylamino-methyl	209
17	5	(*trans*-4-Hydroxy-cyclohexylamino)-carbonyl	>10,000
18	5	(Phenyl-methylamino)-carbonyl	>10,000
19	7	CH_2OH	4.4
20	7	2,2-Dimethyl-propylamino-methyl	34
21	7	2-Hydroxy-ethylamino-methyl	12
22	7	(2-*N*,*N*-Dimethylamino-ethyl)amino-methyl	5.2
23	7	(2-Pyrrolidin-1-yl-ethylamino)-methyl	7.1
24	7	(2-Hydroxy-ethylamino)-carbonyl	5.0
25	7	Methylamino-carbonyl	2.3
26	7	Morpholin-4-yl-carbonyl	91
27	8	OH	671

[a] The compounds were synthesized in the same fashion as those with substitutions at the 6-position.

Table 3. Bis-substitutions at 6- and 7-positions

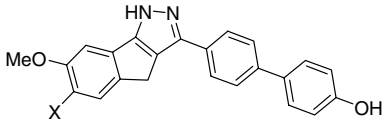

Compound	X	CHK-1 IC_{50} (nM)
33	(4-Hydroxy-piperidin-1-yl)-carbonyl	0.24
34	(4-Methyl-piperazin-1-yl)-carbonyl	2.3
35	(2-Pyrrolidin-1-yl-ethylamino)-carbonyl	0.83
36	(*trans*-4-Hydroxy-cyclohexylamino)-carbonyl	0.24
37	Morpholin-4-yl-carbonyl	0.55
38	2-Hydroxy-ethylamino-methyl	0.43
39	(4-Methyl-piperazin-1-yl)-methyl	0.51
40	(2-Pyrrolidin-1-yl-ethylamino)-methyl	0.21
41	(*trans*-4-Hydroxy-cyclohexylamino)-methyl	0.56
42	(4-Hydroxy-piperidin-1-yl)-methyl	1.1

for an inhibitor in the presence of doxorubicin (150 nM), a DNA-damaging agent. For the combination study, the base line of the regression for EC_{50} calculation was adjusted to the inhibition level determined for 150 nM doxrubicin alone, a concentration known to cause G2/M arrest in HeLa cells. The ratio of the two corresponding EC_{50}s (combo/single) represents a relative potentiation scale of a CHK-1 inhibitor to sensitize doxorubicin. The mechanism for the anti-proliferative function of the inhibitors was examined by a cell cycle analysis (FACS assay) in H1299 cells. The EC_{50} values were measured for an inhibitor alone and also for an inhibitor in combination with doxorubicin. The latter value indicates how effectively an inhibitor can reduce the doxorubicin-induced G2/M cell population. The cellular activity profiles for a group of potent CHK-1 inhibitors are summarized in Table 4 where compounds such as **7** and **36** represent the desirable profiles. These examples had no single agent activity (i.e., not cytotoxic) in either assay (EC_{50} > 22 μM in MTS, EC_{50} > 10 μM in FACS). In combination with doxorubicin, however, they were able to potentiate the anti-proliferative effect of doxorubicin in the MTS assay by a large margin (92-fold for **7** and at least 47-fold for **36**). Meantime, the results from the FACS assay confirmed that the observed potentiation effect was through abrogating G2/M cell arrest with combo-EC_{50} values at 1.3 and 0.61 μM for **7** and **36**, respectively. Some compounds (**9**, **15**, and **19**) showed very weak anti-proliferative potentials, while others (**6**, **12**, **23**, **33**, **40**, and **41**) displayed desirable doxorubicin sensitization but appeared to exhibit single agent cyto-toxicity (EC_{50} value between 0.62 and 2.8 μM in the MTS assay), an indication of certain off-target activities. The clinical implications of single agent activity remain unknown at this stage. It is noteworthy to mention that a lack of good correlation between the intrinsic enzymatic potency and the functional cellular potency was observed. In the literature,[12] some CHK-1 inhibitors have shown diminished cellular activities due to their poor kinase selectivity profile. This

Table 4. Cellular activity of selected CHK-1 inhibitors

Compound	MTS assay EC_{50} (μM)		FACS assay EC_{50} (μM)	
	Single	With Dox[a]	Single	With Dox
6	1.7	1.2	>10	>10
7	23	0.25	>10	1.3
9	>59	28	NT[b]	NT
11	>59	3.6	>10	5.4
12	1.7	0.56	>10	1.6
13	>59	3.3	>10	2.0
15	>59	>5.9	NT	NT
19	>59	8.0	>10	5.5
22	>59	2.5	>10	>10
23	2.8	1.4	NT	NT
33	1.4	0.73	5.2	0.89
36	>59[c]	0.89	>10	0.61
40	0.91	0.19	5.1	1.8
41	0.62	0.27	3.1	1.0
48[d]	8.6	>5.9	>10	2.6

[a] Doxorubicin.
[b] Not tested.
[c] Second test result is 38.
[d] IC_{50} = 18 nM.

class of CHK-1 inhibitors, however, is generally selective against other Ser/Thr kinases as reported earlier.[4] Low cellular activities of compounds with high inhibitory potency may reflect their improper physicochemical properties.

Based on the above assay profiles, compounds **6**, **7**, and **36** were selected for PK evaluation in mice. As shown in Table 5, both mono-substituted compounds, **6** and **7**, had high plasma clearance (CL), moderate-to-large volumes of distribution (V_d), and short half-lives. Both compounds exhibited moderate plasma exposure when dosed intraperitoneally with AUC values being 2.7 μg h/mL for **6** and 4.4 μg h/mL for **7**. However, the oral bioavailability was poor for both. The bis-substituted compound **36** showed even higher clearance and volume of distribution while its oral bioavailability was reduced to an undetectable level. Noticeably, all three compounds are highly lipophilic with clog *P* (ACD) values ranging from 4.8 to 6.0.

In an attempt to further evaluate other factors potentially associated with PK of these molecules, we investigated the solubility, permeability, and metabolism properties of selected compounds. The solubilizing side-chains of **6** and **7** had only marginal impact on aqueous solubility at neutral pH. Both compounds possessed solubility less than 0.03 μg/mL. Although the inadequate water solubility may not be the only reason for the poor oral bioavailability, we made an effort to improve solubility via disrupting the planarity of the tricyclic pyrazole core by preparing the C4 gem-dimethylated compound **48** (Scheme 3). It was observed that this change of geometry did bring a 10-fold boost in aqueous solubility after a direct comparison between the two compounds having similar side-chains as **36**/**48** (data not shown). Unfortunately, the addition of the gem-dimethyl moiety resulted in less enzymatic activity of the inhibitor (IC_{50} = 0.24 nM for **36**, 18 nM for **48**), but more importantly, also diminished the cellular anti-proliferative activity of the compound (combo-EC_{50} in MTS assay more than 5.9 μM as compared to 0.89 μM for **36**, Table 4).

Table 6. Metabolic stability and permeability profile of **7**

Rat liver microsomal stability[a]			Caco-2[b]
$T_{1/2}$ (min)	$K_{elimination}$ (1/min)	% Remaining (30 min)	P_{app} (1×10^{-6} cm/s) (A to B)
25 ± 8	0.0294 ± 0.0100	40 ± 11	13.26 ± 1.36

[a] 1 μM compound concentration, 0.1 mg/mL protein concentration.
[b] 1 μM compound concentration.

The in vitro whole-cell permeability of **7** was assessed via a Caco-2 assay. The apparent permeability (apical to basal) is 13.3×10^{-6} cm/s (Table 6), suggesting that the molecule should have moderate absorption.[13] In the presence of rat liver microsomes, compound **7** showed a half-life of 25 min (Table 6). Major routes of hepatic metabolism included oxidation of the tricyclic/biphenyl rings (data not shown). As reported earlier,[14] the metabolic stability of compounds containing phenol can be enhanced by installing electron-withdrawing groups next to the phenolic hydroxyl group to reduce glucuronidation (phase II metabolism). In addition, this strategy also has the potential to reduce the oxidative metabolism (phase I metabolism) on the aromatic rings due to reduced electron density. To this end, compounds

Table 5. Pharmacokinetic profiles

Compound	CHK-1 IC_{50} (nM)	Mouse iv[a]				Mouse ip[b]		Mouse po[c]		
		CL (L/h kg)	V_d (L/kg)	$T_{1/2}$ (h)	AUC (μg h/mL)	C_{max} (μM)	AUC (μg h/mL)	C_{max} (μM)	AUC (μg h/mL)	*F* (%)
7	9.3	5.4	4.7	0.60	1.2	2.0	4.4	0.25	0.16	4
49	27	3.6	2.4	0.46	1.7	2.8	3.8	<0.05	0	0
50	9091	—	—	—	—	—	—	—	—	—
6	24	4.7	3.4	0.50	1.5	1.1	2.7	0.09	0.45	9
51	28	11	9.2	0.60	0.69	1.3	1.6	0.08	0.13	6
52	>10,000	—	—	—	—	—	—	—	—	—
36	0.24	11	6.0	0.39	0.57	1.5	4.2	<0.1	0	0

[a] Intravenous dosing, 3.0 mg/kg.
[b] Intraperitoneal dosing, 10 mg/kg.
[c] Oral dosing, 10 mg/kg.

with fluoro and cyano groups ortho to the phenolic hydroxyl group were prepared (**49**–**52**, Scheme 4). The data in Table 5 revealed that, compared to the parent molecules (**7** and **6**), compounds with the fluoro substitution (**49** and **51**) maintained the enzymatic inhibition level but the overall PK parameters were generally the same, if not worse. The cyano group, however, was not tolerated in the binding pocket since the resulting compounds (**50** and **52**) lost their inhibitory activity. It is speculated that the combination of poor aqueous solubility and high lipophilicity of the molecules has led to the poor PK profiles. The high lipophilicity may have additionally contributed to the high clearance rate.

In summary, we have systematically studied the substitution patterns on the phenyl ring of the tricyclic core. The substitutions at the 6- or 7-position were more tolerated than positions 5 and 8. The 5-position could only accommodate smaller groups, while even minor substitution at the 8-position led to significant potency loss. Bis-substitution at both the 6- and 7-positions generally led to compounds with higher enzymatic potency (IC_{50} value mostly below 1 nM), while the most potent compounds (**33**, **36**, and **40**) exhibited IC_{50} values between 0.2 and 0.3 nM. The best compound, **36**, was able to potentiate the anti-proliferative effect of doxorubicin in the MTS assay by at least 47-fold. Its mechanism of action was through the abrogation of the cell cycle arrest at the G2/M phase based on the FACS analysis. PK studies in mice revealed that this class of CHK-1 inhibitors had high clearance, moderate bioavailability when dosed intraperitoneally, but poor oral bioavailability. Attempts have been made to analyze the causes for the inadequate PK profiles and specific compounds were synthesized accordingly. While the strategy to improve solubility via disruption of planarity was successful, weaker cellular potency prevented advancement of these analogs. Substituting electron-withdrawing groups such as fluoro next to the phenolic hydroxyl group to potentially alleviate metabolism did not help to improve the PK. It is likely that the combination of low aqueous solubility and high lipophilicity was the primary culprit for the deficient oral bioavailability. In order to address these issues, our future work will call for more dramatic changes to the structure of the molecules including identifying new moieties to replace the lipophilic bi-aryl phenol, while maintaining hydrogen bond interactions with the polar region of the kinase active site necessary for the high potency.

References and notes

1. For reviews, see (a) Zhou, B. B.; Bartek, J. *Nat. Rev. Cancer* **2004**, *4*, 1; (b) Tao, Z.-F.; Lin, N.-H. *Anti-Cancer Agents Med. Chem.* **2006**, *6*, 377.
2. (a) Xiao, Z.; Chen, Z.; Gunasekera, A. H.; Sowin, T. J.; Rosenberg, S. H.; Fesik, S.; Zhang, H. *J. Biol. Chem.* **2003**, *278*, 21767; (b) Mailand, N.; Falck, J.; Lukas, C.; Syljuåsen, R. G.; Welcker, M.; Bartek, J.; Lukas, J. *Science* **2000**, *288*, 1425; (c) Zhao, H.; Watkins, J. L.; Piwnica-Worms, H. *Proc. Natl. Acad. Sci. U.S.A.* **2002**, *99*, 14795.
3. (a) Powell, S. N.; DeFrank, J. S.; Connell, P.; Eogan, M.; Preffer, F.; Dombkowski, D.; Tang, W.; Friend, S. *Cancer Res.* **1995**, *55*, 1643; (b) Kuerbitz, S. J.; Plunkett, B. S.; Walsh, W. V.; Kastan, M. B. *Proc. Natl. Acad. Sci. U.S.A.* **1992**, *89*, 7491.
4. Tong, Y.; Claiborne, A.; Stewart, K. D.; Park, P.; Kovar, P.; Chen, Z.; Credo, R. B.; Gu, W.-Z.; Gwaltney, S. L., II; Judge, R. A.; Zhang, H.; Rosenberg, S. H.; Sham, H. L.; Sowin, T. J.; Lin, N. H. *Bioorg. Med. Chem.* **2007**, *15*, 2759.
5. Doyle, K.; Rafferty, P.; Steele, R.; Turner, A.; Wilkins, D.; Arnold, L. Therapeutic agents. US 6297238.
6. Yin, J.; Buchwald, S. L. *Org. Lett.* **2000**, *2*, 1101.
7. Anastasis, P.; Brown, P. E. *J. Chem. Soc. Perkin Trans. 1* **1982**, 2013.
8. Compounds **8** and **9** were synthesized from known starting materials, 5-hydroxy-2,3-dihydro-1*H*-inden-1-one and 3-iodo-1,4-dihydroindeno[1,2-*c*]pyrazole-6-carbaldehyde, respectively, following similar procedures shown in this article.
9. *CHK-1 enzymatic inhibition assay*. The assay was carried out using a recombinant CHK-1 kinase domain protein with amino acids from residue 1–289. A human biotinylated Cdc25C peptide was used as the substrate (Synpep Catalog# 02-1-22-1-ABB). The reaction mixture contained 25 mM of HEPES at pH 7.4, 10 mM $MgCl_2$, 0.08 mM Triton X-100, 0.5 mM DTT, 5 μM ATP, 4 nM ^{33}P ATP, 5 μM Cdc25C peptide substrate, and 5 nM of the recombinant CHK-1 protein. For potent compound with K_i below 1 nM, 0.5 nM of the recombinant CHK-1 protein and 8 nM of ^{33}P were used. The concentration of the vehicle, DMSO, in the final reaction is 2%. After 30 min at room temperature, the reaction was stopped by the addition of equal volume of 4 M NaCl and 0.1 M EDTA (pH 8.0). A 40 μL aliquot of the reaction mixture was added to a well in a Flash Plate (NEN Life Science Products, Boston, MA) containing 160 μL of phosphate-buffered saline (PBS) without calcium chloride and magnesium chloride and incubated at room temperature for 10 min. The plate was then washed three times in PBS with 0.05% of Tween 20 and counted in a Packard TopCount counter (Packard BioScience Company, Meriden, CT).
10. See Ref. 4 for detailed X-ray co-crystal structures with coordinated deposited in the PDB.
11. See Ref. 4 for assay conditions and representative raw data.
12. Fraley, M. E.; Steen, J. T.; Brnardic, E. J.; Arrington, K. L.; Spencer, K. L.; Hanney, B. A.; Kim, Y.; Hartman, G. D.; Stirdivant, S. M.; Drakas, B. A.; Rickert, K.; Walsh, E. S.; Hamilton, K.; Buser, C. A.; Hardwick, J.; Tao, W.; Beck, S. C.; Mao, X.; Lobell, R. B.; Sepp-Lorenzino, L.; Yan, Y.; Ikuta, M.; Munshi, S. K.; Kuo, L. C.; Kreatsoulas, C. *Bioorg. Med. Chem. Lett.* **2006**, *16*, 6049.
13. Yee, S. *Pharm. Res.* **1997**, *14*, 763.
14. Madsen, P.; Ling, A.; Plewe, M.; Sams, C. K.; Knudsen, L. B.; Sidelmann, U. G.; Ynddal, L.; Brand, C. L.; Anderson, B.; Murphy, D.; Teng, M.; Truesdale, L.; Kiel, D.; May, J.; Kuki, A.; Shi, S.; Johnson, M. D.; Teston, K. A.; Feng, J.; Lakis, J.; Anderes, K.; Gregor, V.; Lau, J. *J. Med. Chem.* **2002**, *45*, 5755.